Chapter 3

Bernstein's Approximation of Generalized Abel's Integral Equation with Application in Tomography

3.1 Introduction

Integral equations with weakly singular kernel create the base for many evolutionary models in the field of science and engineering. They have a very rich history [3, 4, 98]. Similar equations are first studied by Abel, where he found an equation of the curve such that the time taken by a mass particle (no matter where the particle is placed) to slide under influence of gravity, reaches to the end of the curve at the same time. In 1896, Volterra [98] further studied such equations under the regularity condition. Such equations were later named the Volterra integral equations. Volterra proved that there exists a unique solution $u(\gamma)$ in $C[r,s]$ for continuous kernel $k(\gamma,\delta)$ and continuous $g(\gamma)$ for all $\gamma,\delta \in [r,s]$. The general second kind Volterra integral equation defined on $[r,s]$, can be written as,

$$u(\gamma) = g(\gamma) + \int_r^{\gamma} k(\gamma,\delta)\, u(\delta) d\delta, \qquad \gamma \in (r,s). \tag{3.1}$$

where $k(\gamma, \delta)$ is a kernel which depends on two variables and $g(\gamma)$ is a known function. The Fredholm integral equation of second kind can be defined as,

$$u(\gamma) = g(\gamma) + \int_r^s k(\gamma, \delta)\, u(\delta) d\delta, \qquad \gamma \in (r, s). \tag{3.2}$$

In this paper, an idea is developed to solve the GAIEs given by,

$$a(\gamma) \int_r^\gamma \varphi(\delta) k(\gamma, \delta) d\delta + b(\gamma) \int_\gamma^s \varphi(\delta) k(\gamma, \delta) d\delta = \zeta(\gamma), \ \ \gamma \in (r, s) \tag{3.3}$$

where the function $\varphi(\gamma)$ is unknown which we have to approximate and $a(\gamma), b(\gamma), \zeta(\gamma)$ and $k(\gamma, \delta) = \frac{1}{(\gamma - \delta)^\mu}, 0 < \mu < 1$, is the power kernel of convolution type.

For, $a(\gamma) = 1, b(\gamma) = 0, [r, s] = [0,1]$, above equation, is converted into the standard form of Abel's integral equations defined as,

$$\int_0^\gamma \varphi(\delta) k(\gamma, \delta) d\delta = \zeta(\gamma), \tag{3.4}$$

which is a form of first kind Volterra integral equation.

Abel's equations play an important role in many fields of science. Some of them are stereology, seismology, radio astronomy, satellite photometry, electron emission, molecular scattering, radar ranging, testing of optical fibers [99-103]. Many authors have worked on Abel's and generalized Abel's integral equations. Recently, many authors have employed some numerical methods to approximate the solution of a different form of generalized Abel's integral equations. Some of them are: Bernstein operational matrix [97], homotopy perturbation method [6], VIM [7], HPLTM [30] and collocation method Chapter 2.

In this chapter, Bernstein's polynomials and hybrid Bernstein Block-Pulse functions (HBBPF) coupled with the collocation approach are used to developing the numerical schemes for the integral equation defined by Eq. (3.3). Recently, Bernstein's polynomials have created interest among researchers for the applied problems such as integral equations [104], spectroscopy [27], system of Abel integral equations [105], astronomy [106], system of differential equations of fractional order [107], and isoperimetric constraint fractional variational problem [108]. Recently, Block-Pulse functions perform an important role to solve Lane Emden equations [106], integral equations [109, 110], fuzzy integral equations [111] and Volterra-Fredholm integral equations [112]. Here, an attempt is made using Bernstein and hybrid Bernstein Block-Pulse functions to develop the collocation approach for the GAIEs. This approach is beneficial as we obtain good numerical results using only a few basis functions.

The outline of this chapter is as follows. In section 3.2, we give some introduction of the Bernstein polynomials, HBBPF and Bernstein approximation. Section 3.3 presents the methods which are used to approximate the solution of Eq. (3.3). In section 3.4, we survey convergence analysis for the proposed methods. Numerical experiments are performed in section 3.5 to check the accuracy of the purposed method. Application of Abel inversion is added in section 3.6 and the last section concludes the paper.

3.2 Basic Definitions and Results

Definitions 3.1 [112]. Bernstein basis polynomial over [0,1] is given by,

$$\mathcal{B}_{n,k}(\gamma) = \binom{n}{k}\gamma^k(1-\gamma)^{n-k},\ k = 0, \dots, n. \tag{3.5}$$

For our convenience, we define $\mathcal{B}_{n,k}(\gamma) = 0, k < 0 \; or \; k > n$. Any continuous function φ defined on the interval $[0,1]$ can be approximated as,

$$\mathcal{B}_n\big(\varphi(\gamma)\big) = \sum_{k=0}^{n} \varphi(k/n)\, \mathcal{B}_{n,k}(\gamma), \tag{3.6}$$

We can define shifted nth degree Bernstein polynomials over $[a, b]$ as,

$$\mathcal{B}_{n,k}(\gamma) = \binom{n}{k} \frac{(\gamma-a)^k (b-\gamma)^{n-k}}{(b-a)^n}, k = 0, \dots, n. \tag{3.7}$$

and then the function φ can be approximated as,

$$\mathcal{B}_n(\varphi) = \sum_{k=0}^{n} \varphi(a + (b-a)k/n)\, \mathcal{B}_{n,k}(\gamma). \tag{3.8}$$

Theorem 3.1 [104]. For any continuous function φ defined on the interval $[0,1]$ the Bernstein polynomial approximation of φ defined by,

$$\mathcal{B}_n\big(\varphi(\gamma)\big) = \sum_{k=0}^{n} \varphi(k/n)\, \mathcal{B}_{n,k}(\gamma), \tag{3.9}$$

satisfies,

$$\lim_{n\to\infty} \mathcal{B}_n\big(\varphi(\gamma)\big) = \varphi(\gamma). \tag{3.10}$$

Thus Bernstein polynomial is a way to prove the Weierstrass approximation theorem that states that for any function which is continuous on a bounded interval $[0,1]$ can be approximated uniformly by a sequence of polynomials. This theorem implies that for any continuous function φ and for any $\epsilon > 0$, there exists an n such that,

$$\big\|\mathcal{B}_n\big(\varphi(\gamma)\big) - \varphi\| < \epsilon, \tag{3.11}$$

holds. It has been shown that n satisfies,

$$n > \frac{\|\varphi\|}{\rho^2 \epsilon}, \tag{3.12}$$

where $\|*\|$ sup norm on $[0,1]$ and since φ is uniformly continuous on [0,1], we have for $\gamma, \delta \in [0,1]$ such that $|\gamma - \delta| < \rho$, and $|\varphi(\gamma) - \varphi(\delta)| < \epsilon$ [81].

and the error bound,

$$|\mathcal{B}_n(\varphi(\gamma)) - \varphi| \leq \frac{1}{2n}\gamma(1-\gamma)||\varphi''|| \leq \frac{1}{8n} \| \varphi'' \|, \tag{3.13}$$

from which it follows that,

$$\lim_{n\to\infty} n(B_n(\varphi(\gamma)) - \varphi(\gamma)) = \frac{1}{n}\gamma(1-\gamma)||\varphi''||. \tag{3.14}$$

The Eq. (3.14) establishes the rate of convergence $O(\frac{1}{n})$ for $\varphi \in C^2[0,1]$ [104].

Definitions 3.2 [112]. An M-set of Block-functions $b_m(t)$ for $m = 1,2,\dots,M$ on $[a,b)$ is defined as

$$b_m(t) = \begin{cases} 1, & \gamma \in [p_m, p_{m-1}] \\ 0 & \gamma \notin [p_m, p_{m-1}] \end{cases}, \tag{3.15}$$

where $p_m = \frac{(M-m)a+mb}{M}$. (3.16)

Definitions 3.3 [112]. The HBBPF $\mathscr{b}_{m,k}(\gamma)$ on the interval $[a,b]$ are defined as

$$\mathscr{b}_{m,k}(\gamma) = \begin{cases} \binom{n}{k} \frac{(\gamma - l_{m-1})^k (l_m - \gamma)^{n-k}}{(l_m - l_{m-1})^n}, & \gamma \in [l_m, l_{m-1}] \\ 0 & \gamma \notin [l_m, l_{m-1}] \end{cases}, \tag{3.17}$$

for $m = 1,2,\dots,M$ and $k = 0,1,\dots,n$,

where $l_m = \frac{(M-m)a+mb}{M}$, $\quad m = 1,2,\dots,M.$ (3.18)

3.3 Outline of Method

This section describes the methods to approximate the solution of Eq. (3.3).

3.3.1 Bernstein Polynomials Method (B1): Any unknown function φ can be written in a linear combination of Bernstein basis polynomials as,

$$\mathcal{B}_n\big(\varphi_n(\gamma)\big) = \sum_{k=0}^{n} \varphi_n(k/n)\, \mathcal{B}_{n,k}(\gamma), \qquad t \in [0,1]. \tag{3.19}$$

Here $\varphi_n(k/n)$ are known as Bernstein coefficients which we have to calculate.

To approximate the solution of Eq. (3.3), we consider the following form,

$$\Big(a(\gamma) \int_0^{\gamma} \sum_{k=0}^{n} \varphi_n\left(\frac{k}{n}\right) \mathcal{B}_{n,k}(\gamma) k(\gamma,\delta) d\delta + b(\gamma) \int_{\gamma}^{1} \sum_{k=0}^{n} \varphi_n\left(\frac{k}{n}\right) \mathcal{B}_{n,k}(\gamma) k(\delta,\gamma) d\delta\Big) = \zeta(\gamma), \tag{3.20}$$

In order to find the unknowns, $\varphi_n\left(\frac{k}{n}\right), k = 0,1, \dots n$, we replace γ by $\gamma_k \in [0,1]$, $k = 0,1, \dots n$ and convert Eq. (3.20) into a system of algebraic equations. Now Eq. (3.20) reduces to the form,

$$\mathcal{A}X = \mathcal{B}, \tag{3.21}$$

where,

$$\mathcal{A} = \Big[\Big(a(\gamma_k) \int_0^{\gamma_k} \sum_{i=0}^{n} \varphi_n\left(\frac{i}{n}\right) \mathcal{B}_{n,k}(\gamma_k) k(\gamma_k,\delta) d\delta + b(\gamma_k) \int_{\gamma_k}^{1} \sum_{i=0}^{n} \varphi_n\left(\frac{i}{n}\right) \mathcal{B}_{n,k}(\gamma_k) k(\delta,\gamma_k) d\delta\Big)\Big], \tag{3.22}$$

$$X = \left[\varphi\left(\frac{i}{n}\right)\right]^T, \tag{3.23}$$

$$\mathcal{B} = [\zeta(\gamma_k)]^T, \tag{3.24}$$

where $i, k = 0,1, \dots, n$.

Solving this system of equations given by Eq. (3.21), the approximate solution of the Eq. (3.3) is calculated.

3.3.2 Hybrid Bernstein Block-Pulse Functions Method (B2): This section describes the use of HBBPF approximation of the solution of Eq. (3.3).

Any function $f \in L^2[0,1)$ can be written as,

$$f(\gamma) = \sum_{m=1}^{\infty} \sum_{k=0}^{\infty} p_{m,k} \mathscr{b}_{m,k}(\gamma). \tag{3.25}$$

After truncating it to some finite values n and M, we obtain,

$$f(\gamma) = \sum_{m=1}^{M} \sum_{k=0}^{n} p_{m,k} \mathscr{b}_{m,k}(\gamma) = P^T H(\gamma), \tag{3.26}$$

where,

$$P = [p_{10}, \dots, p_{1n}, p_{20}, \dots, p_{2n}, p_{M1}, \dots, p_{Mn}]^T, \tag{3.27}$$

and,

$$H(\gamma) = \left[\mathscr{b}_{1,0}(\gamma), \dots, \mathscr{b}_{1,n}(\gamma), \mathscr{b}_{2,0}(\gamma), \dots, \mathscr{b}_{2,n}(\gamma), \mathscr{b}_{M,1}(\gamma), \dots, \mathscr{b}_{M,n}(\gamma)\right]^T. \tag{3.28}$$

We approximate φ as,

$$\varphi(\gamma) = \sum_{m=1}^{M} \sum_{k=0}^{n} p_{m,k} \mathscr{b}_{m,k}(\gamma) = P^T H(\gamma). \tag{3.29}$$

where P and $H(\gamma)$ are defined by Eq. (3.27) and Eq. (3.28) respectively.

To solve the Eq. (3.3), put φ from Eq. (3.29) in Eq. (3.3), gives,

$$\Big(a(\gamma)\int_0^{\gamma}\sum_{m=1}^{M}\sum_{k=0}^{n}p_{m,k}\mathscr{b}_{m,k}(\gamma)\,k(\gamma,\delta)d\delta +$$

$$b(\gamma)\int_{\gamma}^{1}\sum_{m=1}^{M}\sum_{k=0}^{n}p_{m,k}\mathscr{b}_{m,k}(\gamma)\,k(\delta,\gamma)d\delta\Big)=\zeta(\gamma), \tag{3.30}$$

or,

$$\sum_{m=1}^{M}\sum_{k=0}^{n}p_{m,k}\left(a(\gamma)\int_0^{\gamma}\mathscr{b}_{m,k}(\gamma)k(\gamma,\delta)d\delta+b(\gamma)\int_{\gamma}^{1}\mathscr{b}_{m,k}(\gamma)k(\delta,\gamma)d\delta\right)=\zeta(\gamma), \tag{3.31}$$

Collocating Eq. (3.31) at $M(n+1)$ points $\gamma_l \in [0,1],\ l=1,2,\dots,M(n+1)$, the above equations reduces to the following linear system of equations,

$$\sum_{m=1}^{M}\sum_{k=0}^{n}p_{m,k}\left(a(\gamma_l)\int_0^{\gamma_l}\mathscr{b}_{m,k}(\gamma_l)k(\gamma_l,\delta)d\delta+b(\gamma_l)\int_{\gamma_l}^{1}\mathscr{b}_{m,k}(\gamma_l)k(\delta,\gamma_l)d\delta\right)=$$

$$\zeta(\gamma_l). \tag{3.32}$$

After solving the above system of equations, we obtained the unknown values $\widetilde{p_{m,k}}$, which are the approximate values of $p_{m,k}$.

3.4 Convergence Analysis

This section includes the results on convergence of the schemes described in the last section and we will estimate an error bound for both schemes. For this, Banach space $X = C[0,1]$ is considered associated with the norm defined as,

$$\| \varphi(\gamma) \| = \max_{0\le\gamma\le1}|\varphi(\gamma)|.$$

Also, we define,

$$\Psi\big(\omega(\gamma)\big)=\int_0^{\gamma}k(\gamma,\delta)\,\omega(\delta)d\delta, \tag{3.33}$$

and $\Psi_1\big(\omega(\gamma)\big) = \int_{\gamma}^{1} k(\delta,\gamma)\,\omega(\delta)d\delta,$ (3.34)

Then Ψ and Ψ_1 are bounded on $[0,1]$, *i.e.*, there exist two constants such that,

$\| \Psi(\omega(x)) \| \leq \mathrm{C} \| \omega(x) \|$ and $\| \Psi_1(\omega(x)) \| \leq \mathrm{C}^1 \| \omega(x) \|$. (3.35)

Refer to Chapter 2 (Lemma 2.1).

3.4.1 Convergence for B1:

Theorem 3.2 Consider that all the functions of Eq. (3.3) belongs to $C[0,1]$ and the kernel $k(\delta,\gamma)$ either belongs to $C[0,1]\times C[0,1]$ or $L^2[0,1)$. Let $\varphi(\gamma)$ and $\mathcal{B}_n\big(\varphi_n(\gamma)\big) = \sum_{k=0}^{n} \varphi_n(k/n)\,\mathcal{B}_{n,k}(\gamma)$ be the exact and approximated solution by scheme 1 of Eq. (3.3) respectively. Then,

$\| \varphi(\gamma) - \mathcal{B}_n\big(\varphi_n(\gamma)\big) \| \leq \left(1 + \frac{(\mathrm{C}\|a(\gamma)\| + \|\mathrm{C}^1 b(\gamma)\|)}{(\mathrm{C}\|a(\gamma)\| - \mathrm{C}^1\|b(\gamma)\|)}\right)\frac{1}{8n} \| \varphi'' \|.$ (3.36)

Proof: Suppose that $\mathcal{B}_n\big(\varphi(\gamma)\big) = \sum_{k=0}^{n} \varphi(k/n)\,\mathcal{B}_{n,k}(\gamma)$ be the best approximation of $\varphi(\gamma)$. Then we have,

$\| \varphi(\gamma) - \mathcal{B}_n\big(\varphi_n(\gamma)\big) \| \leq \| \varphi(\gamma) - \mathcal{B}_n\big(\varphi(\gamma)\big) \| + \| \mathcal{B}_n(\varphi(\gamma)) - \mathcal{B}_n\big(\varphi_n(\gamma)\big) \|.$ (3.37)

From relation given by Eq. (3.13), we obtain,

$\| \varphi(\gamma) - \mathcal{B}_n\big(\varphi(\gamma)\big) \| \leq \frac{1}{8n} \| \varphi'' \|.$ (3.38)

Therefore,

$\| \varphi(\gamma) - \mathcal{B}_n\big(\varphi_n(\gamma)\big) \| \leq \frac{1}{8n} \| \varphi'' \| + \| \mathcal{B}_n(\varphi(\gamma)) - \mathcal{B}_n\big(\varphi_n(\gamma)\big) \|.$ (3.39)

Now, it is enough to estimate a bound for $\| \mathcal{B}_n(\varphi(\gamma)) - \mathcal{B}_n\big(\varphi_n(\gamma)\big) \|$. Theorem 1 implies that for any $\varphi \in C[0,1]$ and for any $\varepsilon > 0$ there exists n such that, $\| B_n(\varphi) - \varphi \| < \varepsilon$.

So, we can write Eq. (3.3) as,

$$a(\gamma) \int_0^\gamma \mathcal{B}_n\big(\varphi(\delta)\big)k(\gamma,\delta)d\delta + b(\gamma) \int_\gamma^1 \mathcal{B}_n\big(\varphi(\delta)\big)k(\delta,\gamma)d\delta = \zeta(\gamma), \tag{3.40}$$

If we substitute $\mathcal{B}_n\big(\varphi_n(\delta)\big)$ instead of $\mathcal{B}_n\big(\varphi(\delta)\big)$ in Eq. (3.40) then RHS is replaced by a new function $\zeta_1(\gamma)$ (say). So, we have,

$$a(\gamma) \int_0^\gamma \mathcal{B}_n(\varphi_n(\delta))k(x,\delta)d\delta + b(\gamma) \int_\gamma^1 \mathcal{B}_n(\varphi_n(\delta))k(\delta,\gamma)d\delta = \zeta_1(\gamma). \tag{3.41}$$

Consequently, we have,

$$a(\gamma) \int_0^\gamma \{\mathcal{B}_n\big(\varphi(\delta)\big) - \mathcal{B}_n\big(\varphi_n(\delta)\big)\}k(\gamma,\delta)d\delta + b(\gamma) \int_\gamma^1 \{\mathcal{B}_n\big(\varphi(\delta)\big) - \mathcal{B}_n(\varphi_n(\delta))\}k(\delta,\gamma)d\delta = \zeta(\gamma) - \zeta_1(\gamma). \tag{3.42}$$

or,

$$\| a(\gamma) \int_0^\gamma \{\mathcal{B}_n\big(\varphi(\delta)\big) - \mathcal{B}_n\big(\varphi_n(\delta)\big)\}k(\gamma,\delta)d\delta + b(\gamma) \int_\gamma^1 \{\mathcal{B}_n\big(\varphi(\delta)\big) - \mathcal{B}_n(\varphi_n(\delta))\}k(\delta,\gamma)d\delta \| \leq \| \zeta(\gamma) - \zeta_1(\gamma) \|. \tag{3.43}$$

Or we can write,

$$\| a(\gamma)\Psi\{\mathcal{B}_n\big(\varphi(\gamma)\big) - \mathcal{B}_n\big(\varphi_n(\gamma)\big)\} + b(\gamma)\Psi_1\{\mathcal{B}_n\big(\varphi(\gamma)\big) - \mathcal{B}_n\big(\varphi_n(\gamma)\big)\} \|$$

$$\leq \| \zeta(\gamma) - \zeta_1(\gamma) \|.$$

Using Lemma 3.1, we obtain,

$$\| \mathcal{B}_n(\varphi(\gamma)) - \mathcal{B}_n(\varphi_n(\gamma)) \| (\mathrm{C}\| a(\gamma) \| - \mathrm{C}^1 \| b(\gamma) \|) \leq \| \zeta(\gamma) - \zeta_1(\gamma) \|.$$

$$\| \mathcal{B}_n(\varphi(\gamma)) - \mathcal{B}_n(\varphi_n(\gamma)) \| \leq \frac{1}{(\mathrm{C}\|a(\gamma)\| - \mathrm{C}^1\|b(\gamma)\|)} \| \zeta(\gamma) - \zeta_1(\gamma) \|. \quad (3.44)$$

For finding a bound for, $\| \zeta(\gamma) - \zeta_1(\gamma) \|$, we assume,

$$a(\gamma) \int_0^\gamma \varphi(\delta) k(\gamma, \delta) d\delta + b(\gamma) \int_\gamma^1 \varphi(\delta) k(\gamma, \delta) d\delta = \zeta(\gamma),$$

and, $a(\gamma) \int_0^\gamma \mathcal{B}_n(\varphi(\delta)) k(\gamma, \delta) d\delta + b(\gamma) \int_\gamma^1 \mathcal{B}_n(\varphi(\delta)) k(\gamma, \delta) d\delta = \zeta_1(\gamma).$

So that,

$$\zeta(\gamma) - \zeta_1(\gamma) = a(\gamma) \int_0^\gamma (\mathcal{B}_n(\varphi(\delta)) - \varphi(\delta)) k(\gamma, \delta) d\delta + b(\gamma) \int_\gamma^1 (\mathcal{B}_n(\varphi(\delta)) - \varphi(\delta)) k(\gamma, \delta) d\delta,$$

$$\| \zeta(\gamma) - \zeta_1(\gamma) \| = \| a(\gamma) \int_0^\gamma (\mathcal{B}_n(\varphi(\delta)) - \varphi(\delta)) k(\gamma, \delta) d\delta + b(\gamma) \int_\gamma^1 (\mathcal{B}_n(\varphi(\delta)) - \varphi(\delta)) k(\gamma, \delta) d\delta \|,$$

Using Lemma 3.1,

$$\| \zeta(\gamma) - \zeta_1(\gamma) \| \leq (\mathrm{C}\| a(\gamma) \| + \| \mathrm{C}^1 b(\gamma) \|) \| \Psi_1 \| \| \mathcal{B}_n(\varphi(\delta)) - \varphi(\delta) \|. \quad (3.45)$$

Now using Eq. (3.13), we obtain,

$$\| \zeta(\gamma) - \zeta_1(\gamma) \| \leq (\mathrm{C}\| a(\gamma) \| + \| \mathrm{C}^1 b(\gamma) \|) \frac{1}{8n} \| \varphi'' \|, \quad (3.46)$$

By Eq. (3.39), (3.44), and (3.46), we conclude the required result.

3.4.2 Convergence for B2:

Theorem 3.3 Consider that all the functions of Eq. (3.1) belongs to $C[0,1]$ and the kernel $k(\delta,\gamma)$ either belongs to $C[0,1]\times C[0,1]$ or $L^2[0,1)$. Let $\varphi(\gamma)$ and $\varphi_{M,n}(\gamma) = \sum_{m=1}^{M}\sum_{k=0}^{n} p_{m,k}\mathscr{b}_{m,k}(\gamma) = P^T H(\gamma)$ be the exact and approximated solution by scheme 2 of Eq. (3.1) respectively. Suppose $\mathrm{C}\| a(\gamma) \| < \mathrm{C}^1\| b(\gamma) \|$. Then,

$$\lim_{n\to\infty} \| \varphi(\gamma) - \varphi_{M,n}(\gamma) \| = 0.$$

Proof: Substituting $\varphi_{M,n}(\gamma)$ in Eq. (3.1), results in

$$a(\gamma)\int_0^{\gamma} \varphi_{M,n}(\delta)k(\gamma,\delta)d\delta + b(\gamma)\int_{\gamma}^{1} \varphi_{M,n}(\delta)k(\delta,\gamma)d\delta = \zeta(\gamma), \tag{3.47}$$

Now we have,

$$a(\gamma)\int_0^{\gamma}(\varphi(\delta) - \varphi_{M,n}(\delta))k(\gamma,\delta)d\delta + b(\gamma)\int_{\gamma}^{1}(\varphi(\delta) - \varphi_{M,n}(\delta))k(\delta,\gamma)d\delta = 0, \tag{3.48}$$

$$\| a(\gamma)\int_0^{\gamma}\Big(\varphi(\delta) - \varphi_{M,n}(\delta)\Big)k(\gamma,\delta)d\delta \|$$

$$-\| b(\gamma)\int_{\gamma}^{1}(\varphi(\delta) - \varphi_{M,n}(\delta))k(\delta,\gamma)d\delta \| \leq 0, \tag{3.49}$$

Using Lemma 3.1, above equation reduces to,

$$\mathrm{C}\| a(\gamma) \|\| \varphi(\gamma) - \varphi_{M,n}(\gamma) \| - \mathrm{C}^1\| b(\gamma) \|\| \varphi(\gamma) - \varphi_{M,n}(\gamma) \| \leq 0,$$

$$(\mathrm{C}\| a(\gamma) \| - \mathrm{C}^1\| b(\gamma) \|) \| \varphi(\gamma) - \varphi_{M,n}(\gamma) \| \leq 0,$$

taking $\tau = \frac{\mathrm{C}^1\|b(\gamma)\|}{\mathrm{C}\|a(\gamma)\|}$, we have,

$$(1-\tau) \| \varphi(\gamma) - \varphi_{M,n}(\gamma) \| \leq 0,$$

since $0 < \tau < 1$, therefore,

$$\lim_{n\to\infty} \| \varphi(\gamma) - \varphi_{M,n}(\gamma) \| = 0. \tag{3.50}$$

3.5 Results, Discussion and Numerical Stability:

In this section, the numerical practice of the proposed method will be done and its veracity will be verified. Also, the stability will be shown by implementing it on the GAIEs with known solutions. We consider three known examples of various type from the literature. In first two examples, the case of GAIEs is considered with different types of solution. The last example is the well-known form of Abel's integral,

$\int_r^\gamma \varphi(\delta) \frac{1}{(\gamma-\delta)^{1/2}} d\delta = \zeta(\gamma)$, which is a special case of GAIEs.

The accuracy of both proposed methods is demonstrated by the maximum absolute error defined by,

$$E = |\varphi(\gamma) - \varphi_n(\gamma)|.$$

Here, $\varphi_n(\gamma)$ is the approximated solution and $\varphi(\gamma)$ is the exact solution of GAIEs.

In the following considered examples, if we rewrite the Eq. (3.1) in operator form as,

$$\chi\big(\varphi(\gamma)\big) = \zeta(\gamma). \tag{3.51}$$

Here, $\varphi(\gamma)$ denotes the exact solution of Eq. (3.51), ${\varphi_n}^\delta(\gamma)$ is the noisy approximated function corresponding to the ε times random error to $\varphi(\gamma)$ such that ${\varphi_n}^\delta(\gamma)$ is the approximate solution of the problem,

$$\chi\big(\varphi(\gamma)\big) = \zeta(\gamma) + \varepsilon\delta. \tag{3.52}$$

$\varphi_n{}^0(\gamma)$ denotes the approximate solution of Eq. (3.52) without noise. ε is a sufficiently small constant and δ is uniform random variable with in $[-1,1]$. By applying the both methods mentioned above for noisy analysis, the solution $\varphi_n{}^\delta(\gamma)$ of Eq. (3.52) is obtained. Each of the test examples are solved and analyzed. The obtained results are demonstrated in the different figures which represents the comparison between,

i. Exact solution $\varphi(\gamma)$, approximate solution without noise $\varphi_n{}^0(\gamma)$, approximate solution with noise $\varphi_n{}^{\delta 1}(\gamma)$ and $\varphi_n{}^{\delta 2}(\gamma)$ with random noise $\delta 1$ and $\delta 2$ respectively.

ii. The approximate solution with random noise $\varphi_n{}^{\delta 1}(\gamma)$ and $\varphi_n{}^{\delta 2}(\gamma)$.

Test example 3.1 In this case, we consider Eq. (3.3) with $a(\gamma) = b(\gamma) = 1$, $k(\gamma, \delta) = \frac{1}{(\gamma-\delta)^{1/5}}$ and

$\zeta(\gamma) = e^{\gamma}\left[(1-\gamma)^{4/5}(\gamma-1)^{-4/5}\left\{\Gamma\left(\frac{4}{5}\right) - \Gamma\left(\frac{4}{5}, \gamma-1\right)\right\} + \left\{\Gamma\left(\frac{4}{5}\right) - \Gamma\left(\frac{4}{5}, \gamma\right)\right\}\right]$, where Γ denotes the Gamma function. This takes the form of GAIEs given in [56, 82]. In this case, the known exact solution is $\varphi(\gamma) = e^{\gamma}$.

In Table 3.1, maximum absolute errors are illustrated by B1 and B2. The obtained maximum absolute errors are also compared with the presented method [97, Chapter 2] of the same problem. Jacobi polynomials based collocation method Chapter 2 and almost Bernstein operational matrix approach [97] are used to approximate the solution of GAIEs. The minimum of maximum absolute errors for above problem in Chapter 2 has order $O(10^{-3})$ for $n = 3$ and $O(10^{-7})$ for $n = 5$ (Table 3.2) and in [97] is of order $O(10^{-5})$. By scheme B2, the achieved maximum absolute error has $O(10^{-9})$ with only $n = 3$ basis polynomials (Table 3.1).

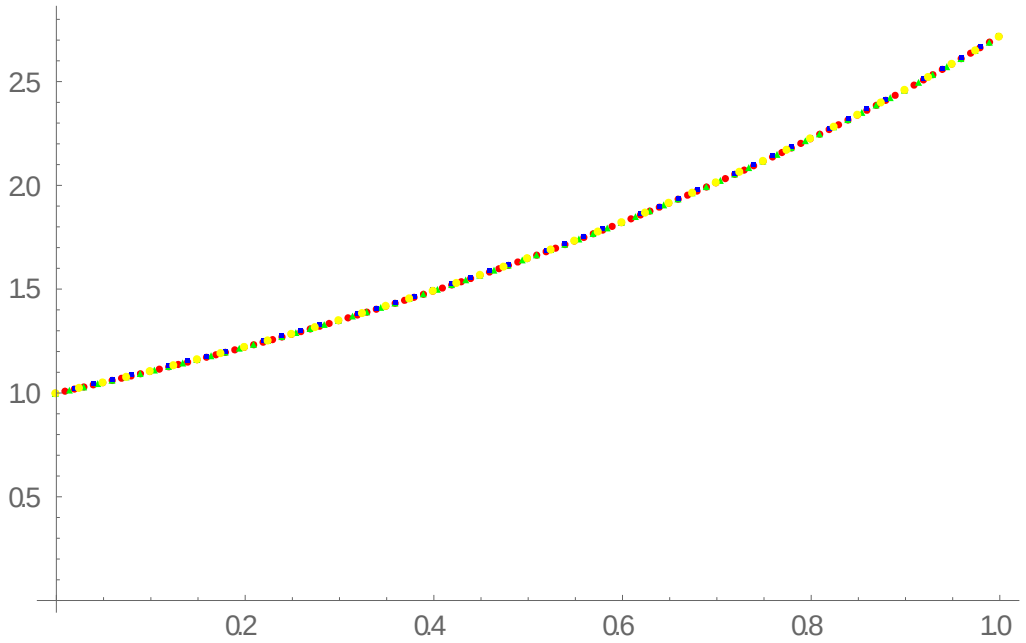

Fig 3.1. Exact solution $\varphi(\gamma)$(red circle), approximate solution without noise ${\varphi_n}^0(\gamma)$ (green triangle), approximate solution with noises ${\varphi_n}^{\delta 1}(\gamma)$ (blue square) and ${\varphi_n}^{\delta 2}(\gamma)$ (yellow circle) for Test example 3.1 by Scheme B1.

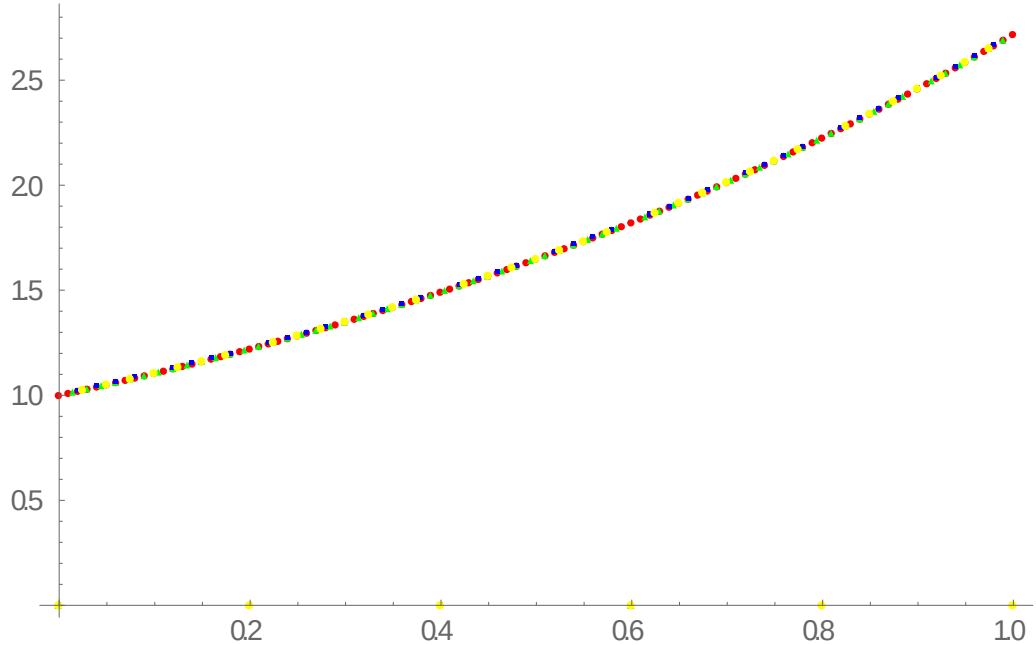

Fig 3.2 Exact solution $\varphi(\gamma)$(red circle), approximate solution without noise ${\varphi_n}^0(\gamma)$ (green triangle), approximate solution with noises ${\varphi_n}^{\delta 1}(\gamma)$ (blue square) and ${\varphi_n}^{\delta 2}(\gamma)$ (yellow circle) for Test example 3.1 by Scheme B2.

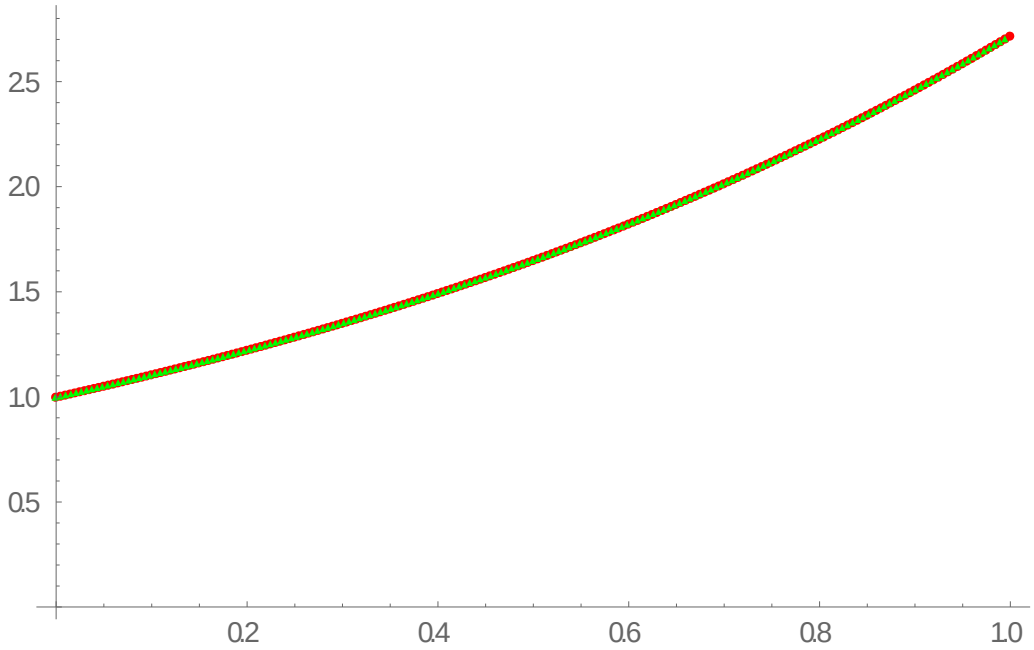

Fig. 3.3 Approximate solutions with noises $\varphi_n{}^{\delta 1}(\gamma)$ (red circle) and $\varphi_n{}^{\delta 2}(\gamma)$ (green triangle) for Test example 3.1 by Scheme B1.

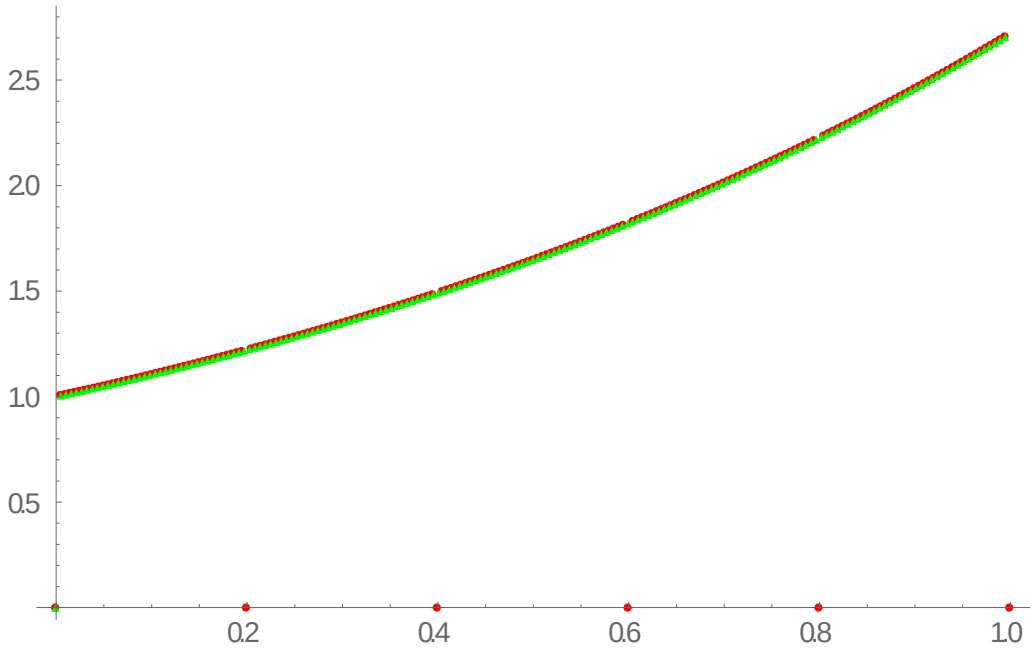

Fig. 3.4 Approximate solutions with noises $\varphi_n{}^{\delta 1}(\gamma)$ (red circle) and $\varphi_n{}^{\delta 2}(\gamma)$ (green triangle) for Test example 3.1 by Scheme B2.

Test example 3.2 This example has been taken from Chapter 2, in which exact solution is in fraction power of γ. For this, we have, $a(\gamma) = b(\gamma) = 1$, $k(\gamma, \delta) = \frac{1}{(\gamma-\delta)^{1/2}}$ and

$$\zeta(\gamma) = \frac{\sqrt{\pi}\gamma^{\frac{5}{6}}\Gamma(-\frac{5}{6})}{\Gamma(-\frac{1}{3})} + \frac{\sqrt{\pi}\gamma^{\frac{5}{6}}\Gamma(\frac{4}{3})}{\Gamma(\frac{11}{6})} + \frac{6}{5}{}_2F_1[-\frac{5}{6}, \frac{1}{2}, \frac{1}{6}, \gamma].$$

For this case, the exact solution is given by $\varphi(\gamma) = \gamma^{1/3}$. This problem is solved by the scheme B1 described in section 3.3 with $n = 1,2,3$ and by scheme B2 with $n = 1,2,3$ and $M = 5,10,15,20$. The obtained maximum absolute errors are shown in Table 3. According to the Table 3.3, we achieved maximum absolute error in order $O(10^{-5})$ which shows the superiority of scheme B2 over B1 and the method presented in Chapter 2 (Table 3.4).

As the exact solution, in this case, is not smooth so scheme B1 doesn't provide the better accuracy and fast convergence (Figure 3.5). This is also clear from Eq. (3.13) which states that the Bernstein approximation converges to the exact solution when the solution is twice continuously differentiable i.e., $\varphi \in C^2[0,1]$. Also, the available methods for GAIEs are failed to achieve an approximation close to the exact solution when the exact solution is not smooth [97, Chapter 2]. This is the beauty of taking the basis functions as hybrid Bernstein polynomial and the approximation converges to exact solution rapidly even when the exact solution is not smooth (Figure 3.6).

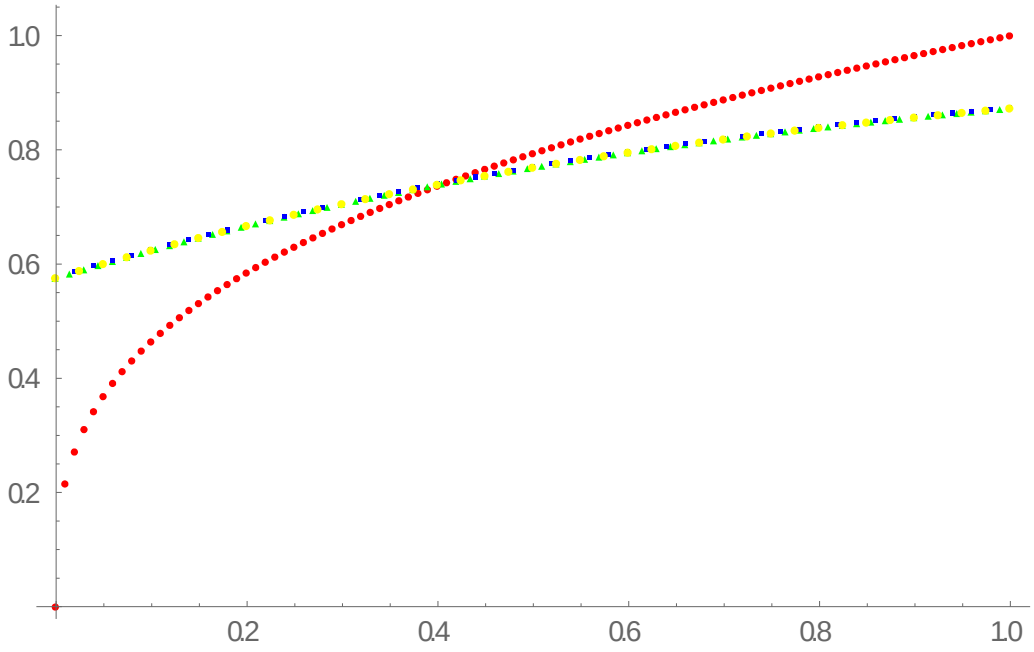

Fig 3.5 Exact solution $\varphi(\gamma)$(red circle), approximate solution without noise ${\varphi_n}^0(\gamma)$ (green triangle), approximate solution with noises ${\varphi_n}^{\delta 1}(\gamma)$ (blue square) and ${\varphi_n}^{\delta 2}(\gamma)$ (yellow circle) for Test example 3.2 by Scheme B1.

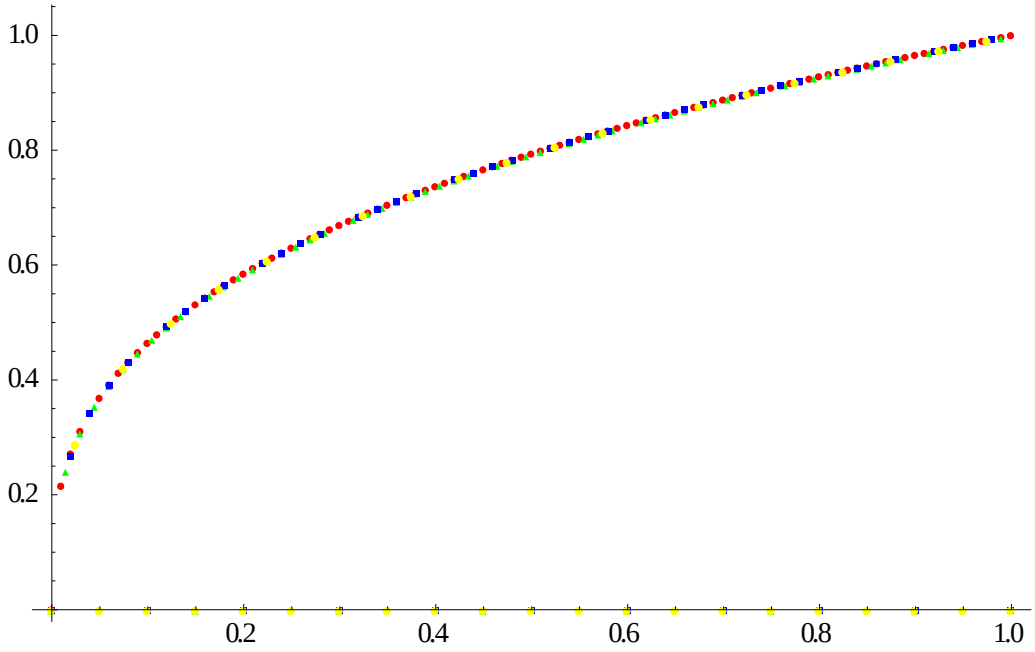

Fig 3.6 Exact solution $\varphi(\gamma)$(red circle), approximate solution without noise ${\varphi_n}^0(\gamma)$ (green triangle), approximate solution with noises ${\varphi_n}^{\delta 1}(\gamma)$ (blue square) and ${\varphi_n}^{\delta 2}(\gamma)$ (yellow circle) for Test example 3.2 by Scheme B2.

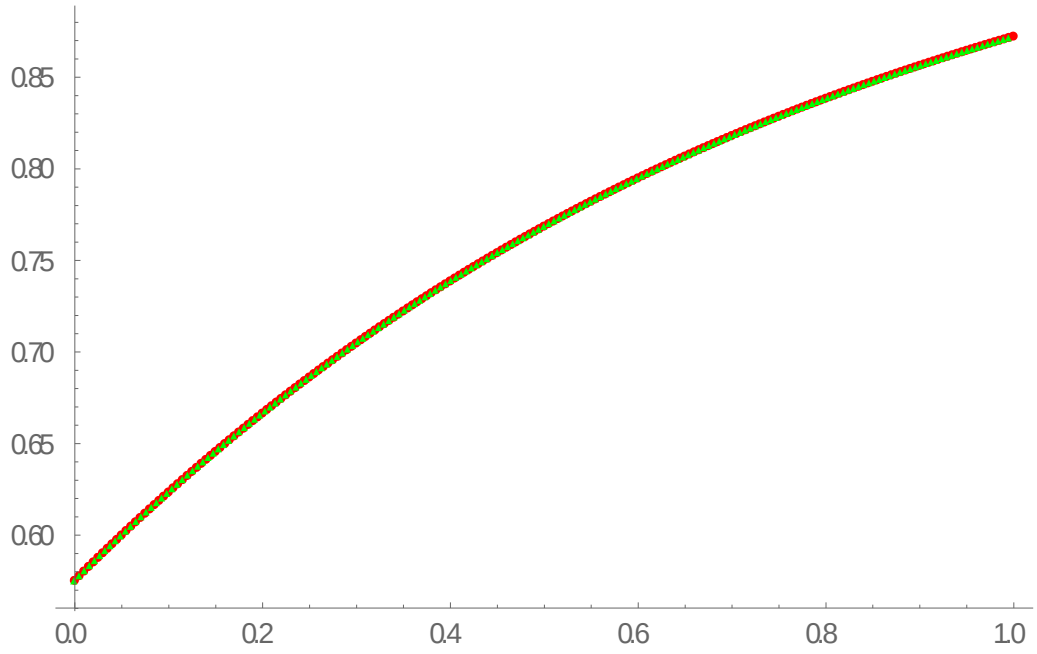

Fig. 3.7 Approximate solutions with noises ${\varphi_n}^{\delta 1}(\gamma)$ (red circle) and ${\varphi_n}^{\delta 2}(\gamma)$ (green triangle) for Test example 3.2 by Scheme B1.

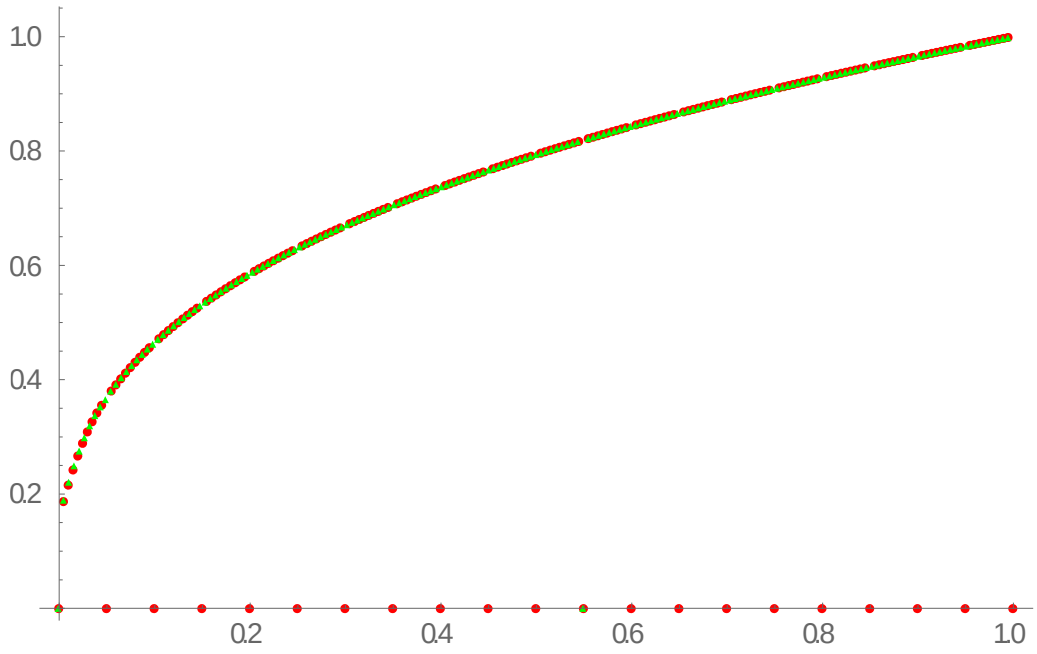

Fig. 3.8 Approximate solutions with noises ${\varphi_n}^{\delta 1}(\gamma)$ (red circle) and ${\varphi_n}^{\delta 2}(\gamma)$ (green triangle) for Test example 3.2 by Scheme B2.

Test example 3.3 Consider [5, 85], $a(\gamma) = 1, b(\gamma) = 0\,, k(\gamma, \delta) = \frac{1}{(\gamma-\delta)^{1/2}}$ and

$\zeta(\gamma) = e^{\gamma} - 1.$

This problem has exact solution $e^{\gamma}\,\mathrm{Erf}[\sqrt{\gamma}]/\sqrt{\pi}$ which is also not smooth. This problem is also solved by B1 and B2 and obtained numerical errors are shown in Table 3.5. It can be observed from Table 3.5 and from figs. 3.9, 3.10 that B2 provides a good approximation over B1 and available methods.

Table 3.1. Maximum absolute error by B1 and B2 for Test example 3.1.

n	$B1$	$S2$			
		$M = 5$	$M = 10$	$M = 15$	$M = 20$
1	0.177	$2.41E-3$	$7.19E-4$	$3.39E-4$	$1.96E-4$
2	$2.94E-2$	$1.48E-4$	$1.89E-5$	$5.61E-6$	$2.35E-6$
3	$1.66E-3$	$2.44E-6$	$1.59E-7$	$3.17E-8$	$9.74E-9$

Table 3.2 Maximum absolute error for Test example 3.1 using different polynomials Chapter 2.

n	*Jacobi*	*Legendre*	*Chebyshev*	*Gegenbauer*
3	$1.667E-3$	$1.667E-3$	$1.667E-3$	$1.667E-3$
5	$4.123E-5$	$2.182E-7$	$1.123E-5$	$1.123E-5$

Table 3.3 Maximum absolute error by B1 and B2 for Test example 3.2.

n	$B1$	$S2$			
		$M = 5$	$M = 10$	$M = 15$	$M = 20$
1	0.193	$2.08E-3$	$2.26E-3$	$9.05E-4$	$5.44E-4$
2	0.119	$6.49E-4$	$3.54E-4$	$1.54E-4$	$7.81E-5$
3	$7.49E-2$	$5.29E-4$	$1.43E-4$	$6.64E-5$	$3.88E-5$

Table 3.4 Maximum absolute error for Test example 3.2 using different polynomials Chapter 2.

n	*Jacobi*	*Legendre*	*Chebyshev*	*Gegenbauer*
3	$7.499E-2$	$7.499E-2$	$7.499E-2$	$7.499E-2$
5	$5.781E-2$	$5.781E-2$	$5.781E-2$	$5.781E-2$

Table 3.5 Maximum Absolute error by B1 and B2 for Test example 3.3.

n	$B1$	$S2$			
		$M=5$	$M=10$	$M=15$	$M=20$
1	0.73	$3.67E-4$	$3.09E-4$	$1.29E-4$	$6.50E-5$
2	$1.35E-2$	$3.15E-4$	$6.29E-5$	$2.23E-5$	$9.49E-6$
3	$9.42E-2$	$1.48E-4$	$1.13E-5$	$5.28E-6$	$1.66E-6$

3.6 Application in Tomography:

The interior of an object was imaged by Abel [4] in terms of inversion in 1826, which resulted in Abel inversion techniques. Abel analytically solved the inversion of a cylindrically symmetric object. Before the invention of x-rays, there was not any developed technique which images the interior of an object. Although the Radon transform is generally used in x-ray tomography. The Radon transform reduces to the Abel transform, which exactly reconstructs a cylindrically symmetrical object from a single x-ray radiograph. However, difficulties in utilizing the Abel transform arise for several reasons that include the physics of x-ray radiography, as well as properties of the Abel transform itself, as it applies to this problem.

Abel transform describes the relationship between the result distribution of the emission coefficient $\varepsilon(r)$ and measured intensity $I(y)$. Reconstruction of the emission coefficient from its projection is known as Abel inversion.

The relation between the emission coefficients $\varepsilon_\lambda(r)$ and intensity $I_\lambda(y)$ can be described as [105],

$$I_\lambda(y) = \int_{-\sqrt{a^2-y^2}}^{\sqrt{a^2-y^2}} \varepsilon_\lambda(r)dr, \tag{3.53}$$

for a specific wavelength λ, here y denotes the displacement of the intensity profile from the line of plasma center, the radial distance from the center of the source $x^2 + y^2 = r^2$is r , and a is the source radius. It is assumed that $\varepsilon_\lambda(r)$ vanishes for $r > a$, and hence $I_\lambda(y)$ vanishes for $mod(y) > a$. For simplicity, we take $a = 1.0$ in Eq. (3.1).

The relation between the emission coefficients $\varepsilon_\lambda(r)$ and intensity $I_\lambda(y)$ can be described as [105],

$$I(y) = 2\int_y^1 \frac{\varepsilon(r).r}{\sqrt{r^2-y^2}}dr. \tag{3.54}$$

By change of variables, Eq. (3.54) reduces to a special case of Eq. (3.3) when $a(\gamma) = 0, b(\gamma) = 1$,

$$\zeta(\gamma) = \int_\gamma^1 \frac{\phi(y)}{\sqrt{\gamma-y}}dy, \tag{3.55}$$

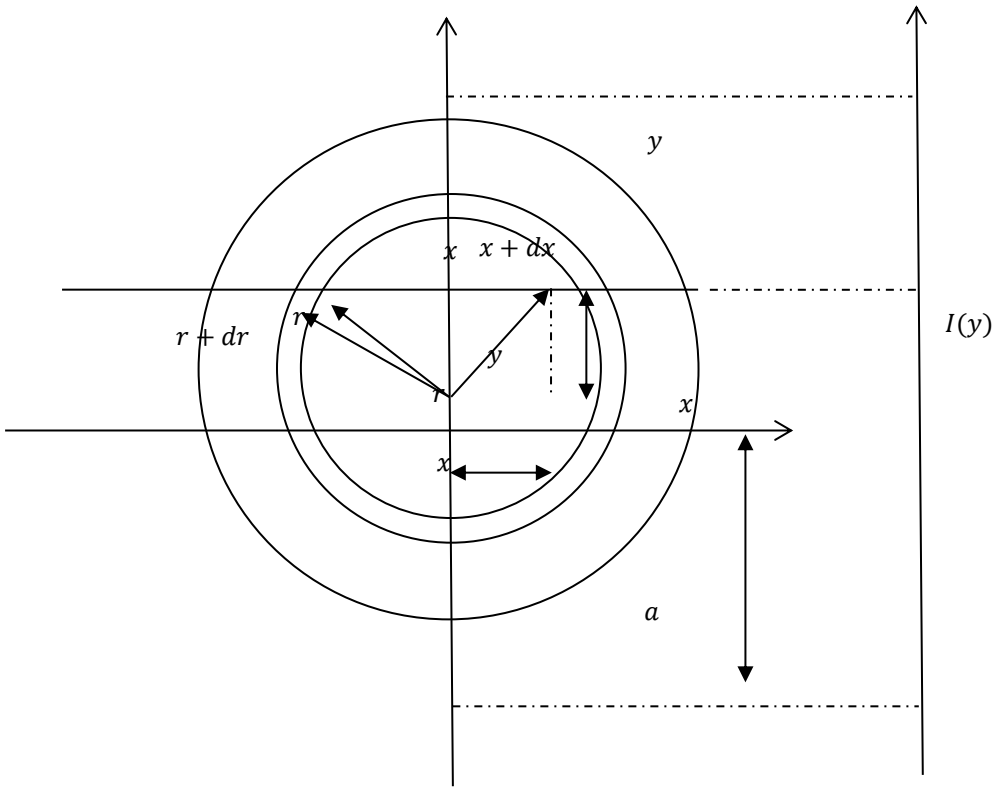

Fig. 3. A Geometrical interpretation of the Abel transform in two dimensions with radius a [105].

where $\zeta(\gamma) = I(\sqrt{\gamma})$ and $\phi(y) = (\varepsilon\sqrt{\gamma})$.

Test example 3.4 Consider Eq. (3.55) with [113, 105]

$$\phi(y) = \frac{1}{2}(1 + 10y - 23y^2 + 12y^3),\ 0 \le y \le 1,$$

$$\zeta(\gamma) = \frac{8}{105}(1-\gamma)^{5/2}(19 + 72\gamma),\ 0 \le \gamma \le 1.$$

We solve this problem with both schemes and obtain numerical results. In this case, the obtained maximum absolute error is $E = 2.868 \times 10^{-16}$ by B1 and $E = 5.270 \times 10^{-15}$ by B2. Also, we solve Test example 3.4, with some random noise. Figures 3.13 and 3.14 illustrates that approximate solutions with and without noise almost coincide. For this

Test examples, we plot the output results (Figs. 3.13-3.16) and also the maximum absolute errors (Figs. 3.17-3.18) which are defined as,

i.) Maximum absolute error E between the exact and approximate solution without noise,

$$E = |\varphi(\gamma) - \varphi_n(\gamma)|.$$

ii.) Maximum absolute error $E1$ between the exact and approximate solution with noise $\delta 1$,

$$E1 = |\varphi(\gamma) - {\varphi_n}^{\delta 1}(\gamma)|.$$

iii.) Maximum absolute error $E2$ between the exact and approximate solution with noise $\delta 2$,

$$E2 = |\varphi(\gamma) - {\varphi_n}^{\delta 2}(\gamma)|.$$

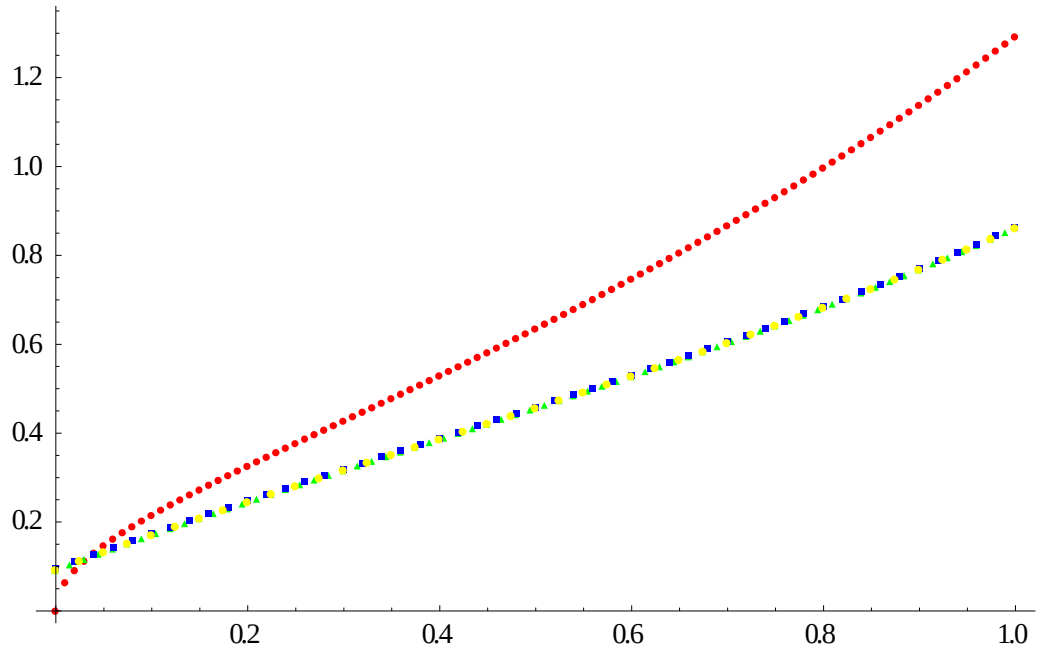

Fig. 3.9 Exact solution $\varphi(\gamma)$(red circle), approximate solution without noise ${\varphi_n}^{0}(\gamma)$ (green triangle), approximate solution with noises ${\varphi_n}^{\delta 1}(\gamma)$ (blue square) and ${\varphi_n}^{\delta 2}(\gamma)$ (yellow circle) for test example 3 by Scheme B1.

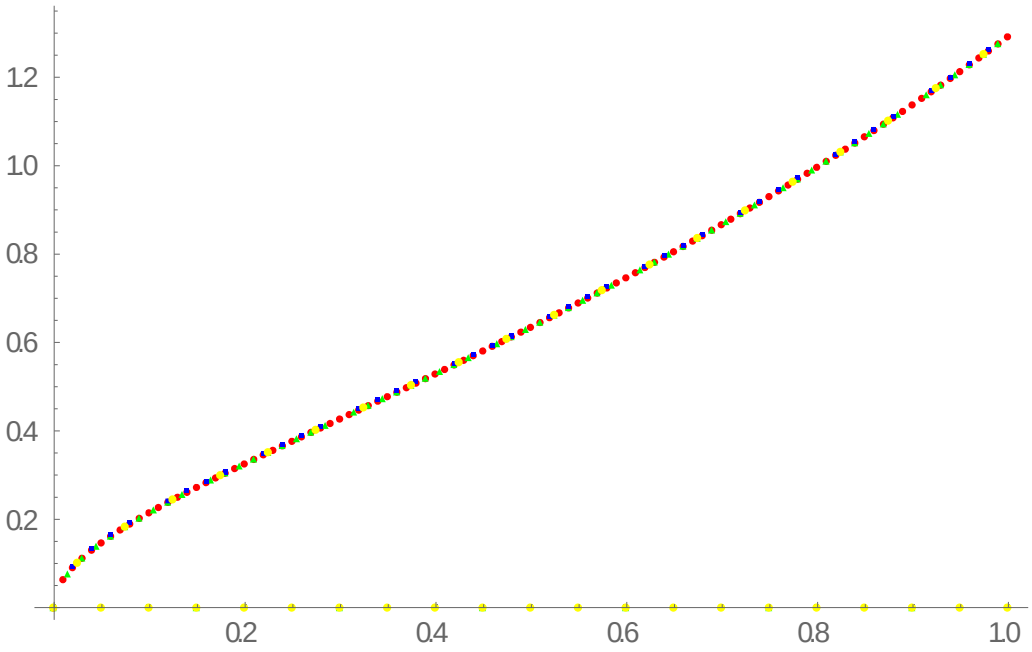

Fig. 3.10 Exact solution $\varphi(\gamma)$(red circle), approximate solution without noise ${\varphi_n}^0(\gamma)$ (green triangle), approximate solution with noises ${\varphi_n}^{\delta 1}(\gamma)$ (blue square) and ${\varphi_n}^{\delta 2}(\gamma)$ (yellow circle) for test example 3 by Scheme B2.

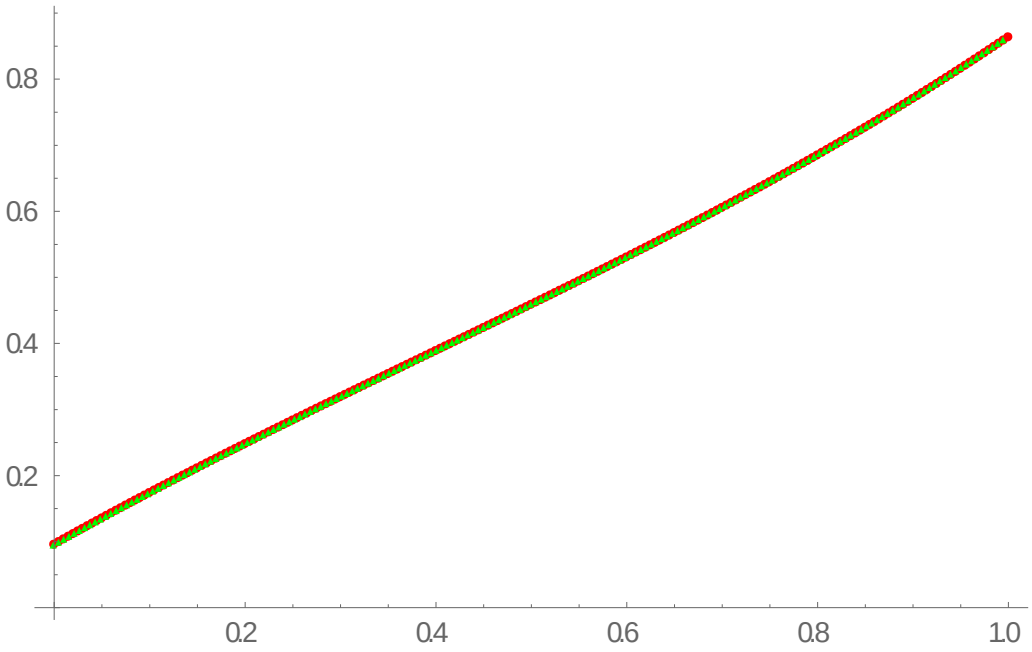

Fig. 3.11 Approximate solutions with noises ${\varphi_n}^{\delta 1}(\gamma)$ (red circle) and ${\varphi_n}^{\delta 2}(\gamma)$ (green triangle) for test example 3 by Scheme B1.

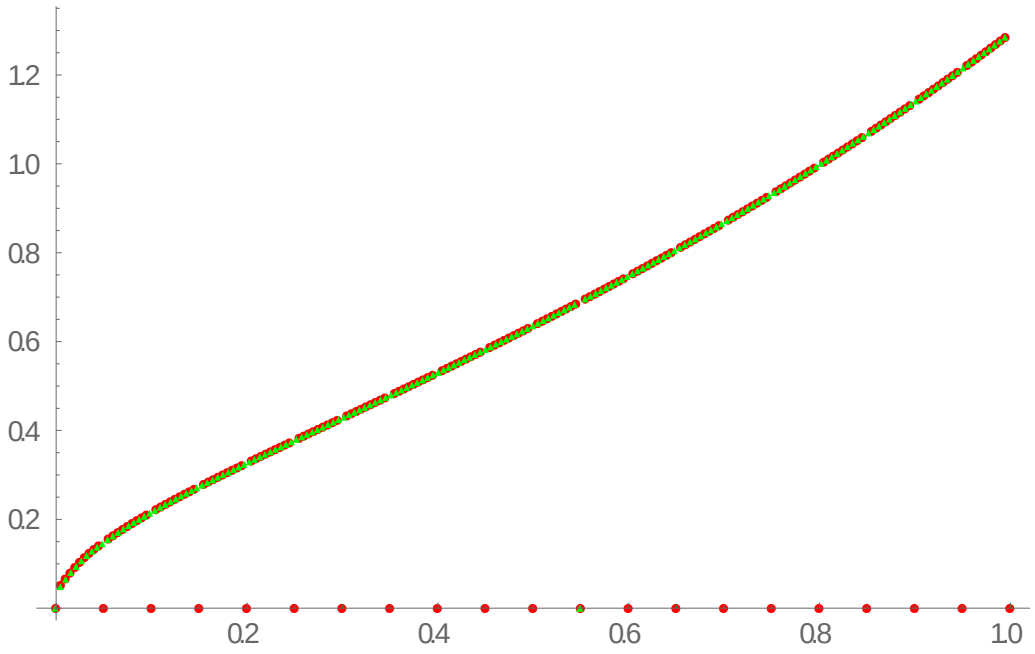

Fig. 3.12 Approximate solutions with noises ${\varphi_n}^{\delta 1}(\gamma)$ (red circle) and ${\varphi_n}^{\delta 2}(\gamma)$ (green triangle) for test example 3 by Scheme B2.

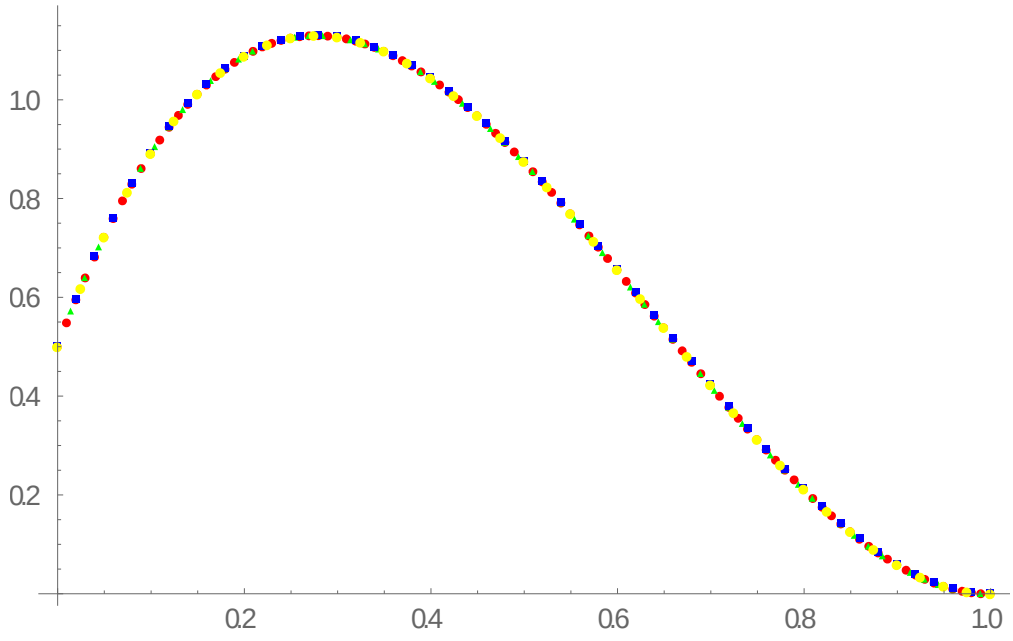

Fig. 3.13 Exact solution $\varphi(\gamma)$(red circle), approximate solution without noise ${\varphi_n}^{0}(\gamma)$ (green triangle), approximate solution with noises ${\varphi_n}^{\delta 1}(\gamma)$ (blue square) and ${\varphi_n}^{\delta 2}(\gamma)$ (yellow circle) for test example 4 by Scheme B1.

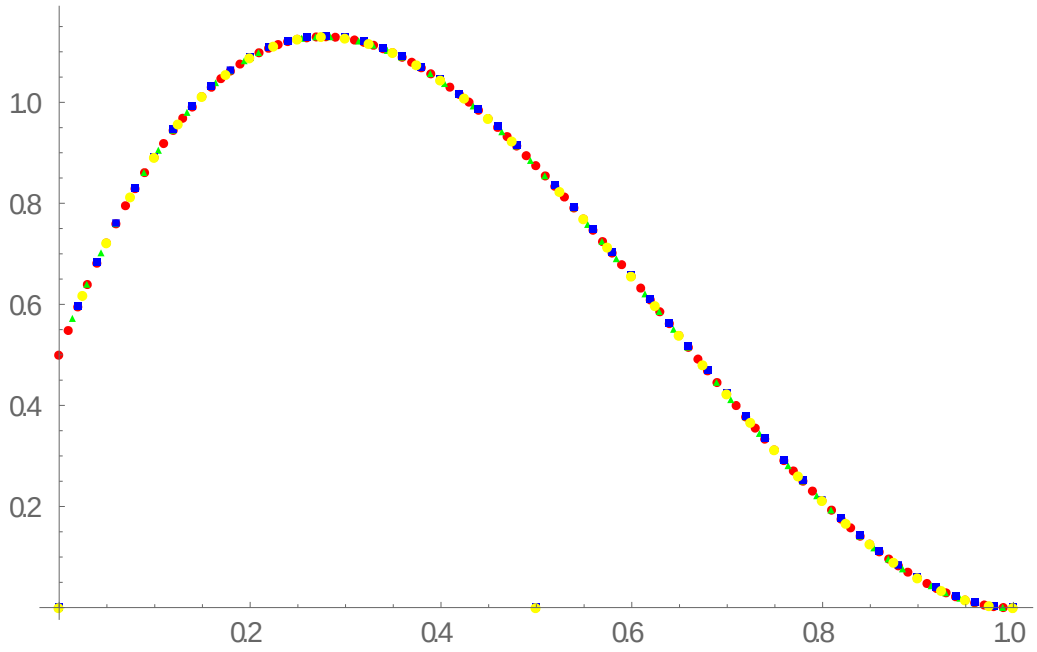

Fig 3.14 Exact solution $\varphi(\gamma)$(red circle), approximate solution without noise ${\varphi_n}^0(\gamma)$ (green triangle), approximate solution with noises ${\varphi_n}^{\delta 1}(\gamma)$ (blue square) and ${\varphi_n}^{\delta 2}(\gamma)$ (yellow circle) for test example 4 by Scheme B2.

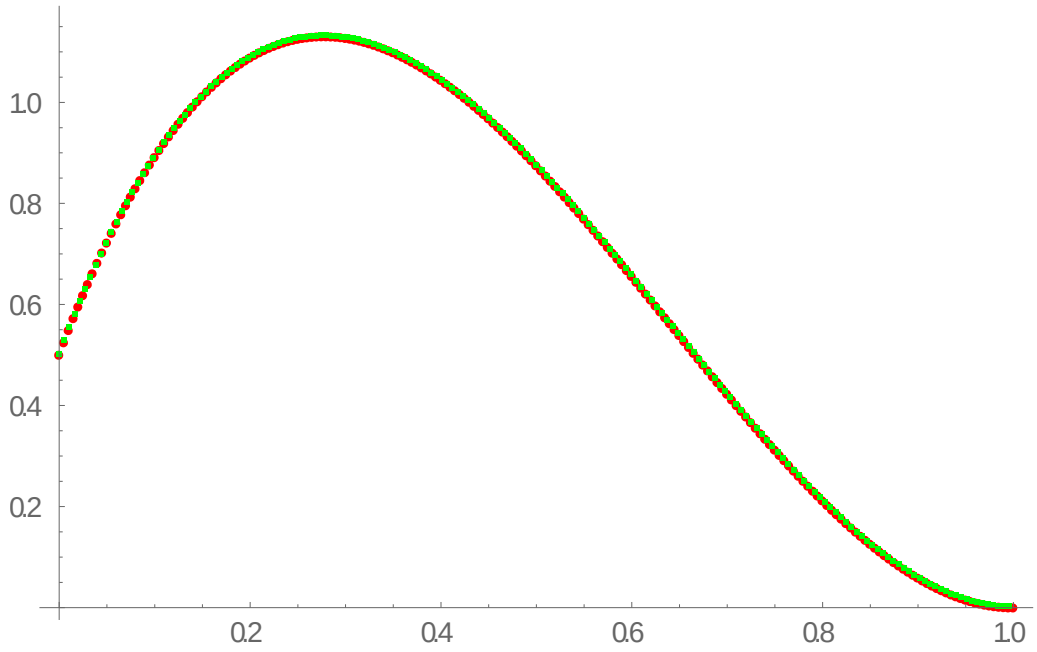

Fig. 3.15 Approximate solutions with noises ${\varphi_n}^{\delta 1}(\gamma)$ (red circle) and ${\varphi_n}^{\delta 2}(\gamma)$ (green triangle) for test example 4 by Scheme B1.

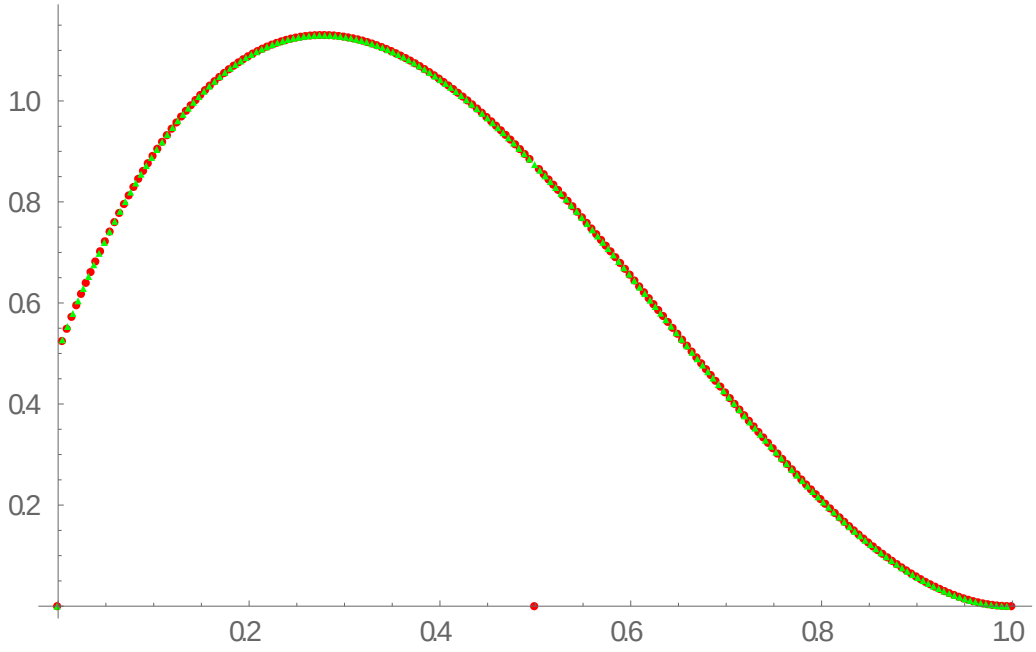

Fig. 3.16 Approximate solutions with noises ${\varphi_n}^{\delta 1}(\gamma)$ (red circle) and ${\varphi_n}^{\delta 2}(\gamma)$ (green triangle) for test example 4 by Scheme B2.

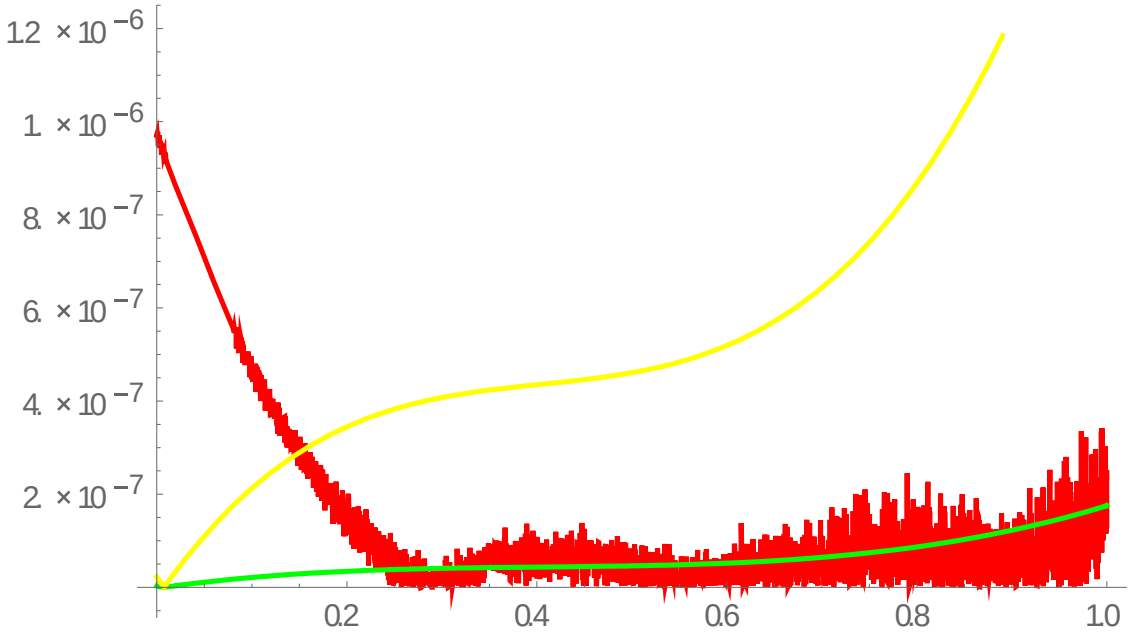

Fig. 3.17 Obtained maximum absolute errors $10^8 E(red)$, $E1(green)$, $10^3 E2(yellow)$ for test example 4 by B1.

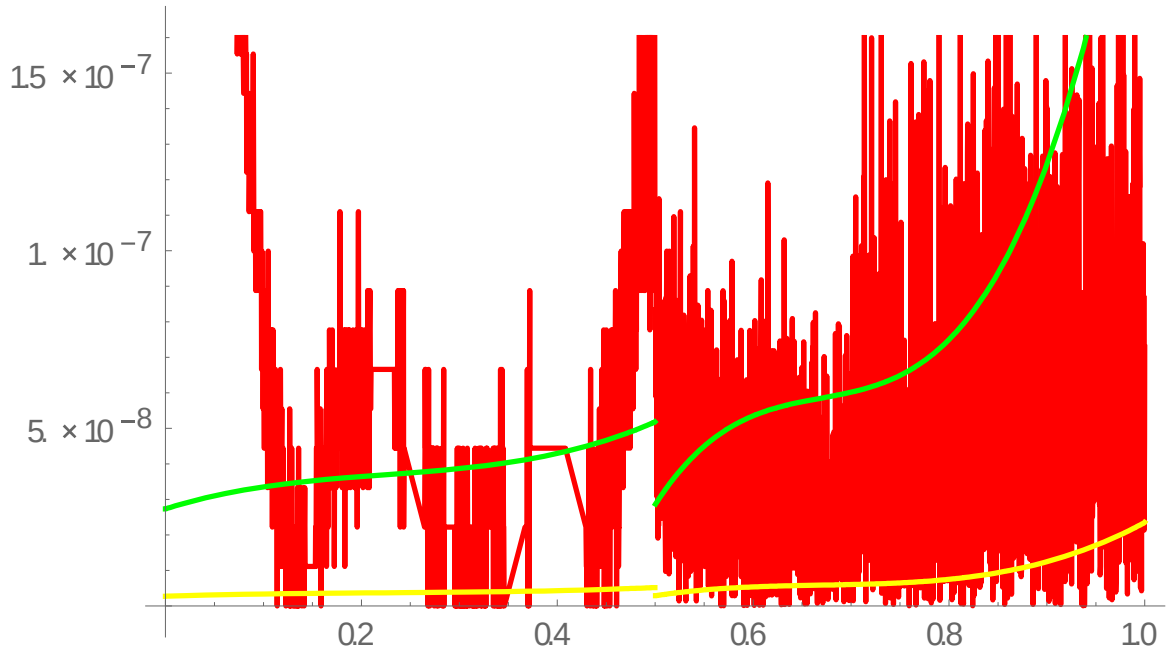

Fig. 3.18 Obtained maximum absolute errors $10^8E(red)$, $E1(green)$, $10^1E2(yellow)$ for test example 4 by B2.

3.7 Conclusion

A new and simple approach based on Bernstein polynomials (scheme 1) is presented coupled with collocation method to approximate the numerical solution of GAIEs. In order to obtain the better accuracy, when the exact solution is not smooth or twice continuously differentiable, hybrid Bernstein Block-Pulse function is used as basis functions (in scheme 2) and better results has been obtained. The simplicity of this method is that it converts the GAIEs into algebraic equations which can be rapidly solved by computation. The theoretical results describing the convergence of the schemes B1 and B2 are also established. Numerical experiments are added to demonstrate the accuracy of lower-order approximations. It has been noticed that both schemes work well and provide better approximation. Moreover, scheme 2 provides better results in comparison of scheme 1 and has very high accuracy. It proves its superiority over the B1 and over available methods in literature [5, 105, 113, Chapter 2].